Biology of Reproduction, 2018, 99(2), 373–383
doi:10.1093/biolre/ioy048
Research Article
Advance Access Publication Date: 22 February 2018

OXFORD

Research Article

Influence of the genetic background on the reproductive phenotype of mice lacking Cysteine-Rich Secretory Protein 1 (CRISP1)†

Mariana Weigel Muñoz[1], María A. Battistone[1,‡], Guillermo Carvajal[1,‡], Julieta A Maldera[1], Ludmila Curci[1], Pablo Torres[2], Daniel Lombardo[2], Omar P. Pignataro[1,3], Vanina G. Da Ros[1] and Patricia S. Cuasnicú[1,*]

[1]Instituto de Biología y Medicina Experimental (IByME-CONICET), Buenos Aires, Argentina; [2]Instituto de Investigación y Tecnología en Reproducción Animal, Facultad de Ciencias Veterinarias, Universidad de Buenos Aires, Buenos Aires, Argentina and [3]Departamento de Química Biológica, Facultad de Ciencias Exactas y Naturales, Universidad de Buenos Aires, Buenos Aires, Argentina

*__Correspondence:__ Instituto de Biología y Medicina Experimental (IByME-CONICET), Vuelta de Obligado 2490, Buenos Aires, C1428ADN, Argentina. E-mail: pcuasnicu@gmail.com

†**Grant support:** This study was partially supported by the WHO (H9/TSA/037), the National Research Council (PIP 2015 N° 149) and the National Agency for Scientific and Technological Promotion (PICT 2015 N° 471) to PSC.
MAB and GC contributed equally to this paper.
‡Edited by Government of Canada, Canadian Institutes of Health Research: Stephen J Lye, 160117; Government of Canada, Canadian Institutes of Health Research: Kristin L Connor, 246638.

Received 21 August 2017; Revised 30 January 2018; Accepted 21 February 2018

Abstract

Epididymal sperm protein CRISP1 has the ability to both regulate murine CatSper, a key sperm calcium channel, and interact with egg-binding sites during fertilization. In spite of its relevance for sperm function, *Crisp1*$^{-/-}$ mice are fertile. Considering that phenotypes can be influenced by the genetic background, in the present work mice from the original mixed *Crisp1*$^{-/-}$ colony (129/SvEv∗C57BL/6) were backcrossed onto the C57BL/6 strain for subsequent analysis of their reproductive phenotype. Whereas fertility and fertilization rates of C57BL/6 *Crisp1*$^{-/-}$ males did not differ from those reported for mice from the mixed background, several sperm functional parameters were clearly affected by the genetic background. *Crisp1*$^{-/-}$ sperm from the homogeneous background exhibited defects in both the progesterone-induced acrosome reaction and motility not observed in the mixed background, and normal rather than reduced protein tyrosine phosphorylation. Additional studies revealed a significant decrease in sperm hyperactivation as well as in cAMP and protein kinase A (PKA) substrate phosphorylation levels in sperm from both colonies. The finding that exposure of mutant sperm to a cAMP analog and phosphodiesterase inhibitor overcame the sperm functional defects observed in each colony indicated that a common cAMP-PKA signaling defect led to different phenotypes depending on the genetic background. Altogether, our observations indicate that the phenotype of CRISP1 null males is modulated by the genetic context and reveal new roles for the protein in both the functional events and signaling pathways associated to capacitation.

Summary Sentence

Analysis of the reproductive phenotype of mice lacking CRISP1 shows the influence of the genetic background on different sperm functional parameters and reveals the involvement of CRISP1 in the cAMP-PKA signaling cascade leading to capacitation.

Key words: sperm, capacitation, fertilization, signal transduction.

Introduction

Mammalian fertilization involves a complex sequence of events beginning with the entrance of millions of spermatozoa into the female reproductive tract and ending with the incorporation of a single spermatozoon into the egg. In order to acquire their fertilizing ability, sperm must undergo two processes known as maturation and capacitation which occur in the male and female tract, respectively. Whereas maturation confers sperm the ability to recognize and fertilize the egg, capacitation prepares the cells for both undergoing the acrosome reaction (AR), an exocytotic event that takes place in the head, and developing a vigorous and intermittent flagellar movement known as hyperactivation (HA). Although evidence revealed that sperm capacitation involves mainly activation of the cAMP/PKA-dependent increase in protein tyrosine (Tyr) phosphorylation (pTyr) [1, 2] as well as an increase in intracellular Ca^{2+} concentrations [3], how these signaling pathways interact to induce AR and HA is still under investigation. The occurrence of these functional events enables penetration of the egg envelopes: the cumulus oophorus and the zona pellucida (ZP), and subsequent fusion with the egg plasma membrane.

In spite of the importance of fertilization, the molecular mechanisms and the identity of the molecules involved in this process are not completely elucidated. In this regard, substantial evidence supports the participation of proteins belonging to the Cysteine-RIch Secretory Protein (CRISP) family in different stages of fertilization [4]. CRISP proteins are characterized by the presence of 16 conserved Cys, 10 of which are located in the C-terminal region containing both a Cysteine-Rich Domain (CRD) and a hinge that connects it to the plant Pathogenesis Related-1 (PR-1) domain located in the N-terminus of the molecule [5]. Evidence indicates that these two domains have different functions. Whereas the N-terminal PR-1 domain has been implicated in membrane interaction and protease activity, the C-terminal region possess ion channel regulatory properties [5–7]. In mammals, four members of the CRISP family have been described (CRISP1, CRISP2, CRISP3, and CRISP4), with a predominant expression in the male reproductive tract [4]. Our laboratory identified, characterized, and purified the first member of this family, namely CRISP1 [8–10], a major glycoprotein secreted by the epididymis in response to androgens that associates with the sperm surface with two different affinities during maturation [11, 12]. Whereas the loosely bound population was proposed to act as a decapacitating factor regulating protein pTyr and the progesterone-induced AR [13], the tightly bound population was reported to have a role in both sperm–ZP interaction and gamete fusion through its interaction with complementary sites localized in the ZP and the oolema, respectively [14–16]. These last results were confirmed by using CRISP1 knockout mice generated in our laboratory [17]. Interestingly, recent observations showed that CRISP1 is also present in the cumulus cells that surround the egg and modulates both sperm HA and orientation very likely through its ability to regulate CatSper [18], the principal sperm Ca^{2+} channel involved in HA development and essential for male fertility [19–21].

Table 1. Fertility of B6 CRISP1-deficient males.

	Control	*Crisp1* $^{-/-}$
% pregnant females	**79.2 ± 7.2**	**81.3 ± 6.3**
Average litter size	**5.3 ± 1.3**	**5.9 ± 0.6**

Data represents the mean ± SEM of 7 males. ns.

The mouse line deficient in CRISP1 used in our studies was generated in a mixed 129/SvEv∗C57BL/6 background [17]. *Crisp1*$^{-/-}$ spermatozoa from this colony exhibited normal sperm motility and progesterone-induced AR rates but clear defects in protein pTyr and in their ability to interact with both the ZP and the oolema. In spite of these defects, CRISP1-deficient mice were fertile [17]. The finding that different functional deficiencies in *Crisp1*$^{-/-}$ spermatozoa were not sufficient to affect the fertility of the knockout males has also been observed in numerous sperm protein knockout models [22]. One possible explanation for these observations is that mouse phenotypes are not entirely controlled by the mutation at the targeting locus but are modulated by the genetic background at other loci [23]. This idea is supported by substantial evidence indicating that a single gene mutation can produce markedly different phenotypes depending on the genetic background of the animals [24, 25]. It has been reported that disruption of tetraspanin CD81, *Smcp* (mitochondria sperm protein associated cysteine rich) or *Ldhc* (lactate dehydrogenase type C) genes could result in infertility, subfertility, or normal fertility depending on the mouse strain [26–29]. Furthermore, strain-specific effects have been observed on several sperm functional parameters that are affected differently depending on the background of the animal [29, 30]. Based on this, in the present work we analyzed the influence of the genetic background on the reproductive phenotype of male mice lacking CRISP1.

Materials and Methods

Animals

Mice lacking CRISP1, originally generated in a mixed 129/SvEv∗C57BL/6 background [17], were backcrossed onto the C57BL/6 strain for 10 generations to reach at least 99.95% homogeneity. Animals were maintained with food and water ad libitum in a temperature controlled room with a 12:12 hour light: dark cycle. Approval for the study protocol (CE 036-June 2014) was obtained from the Bioethics Committee of the Institute of Biology and Experimental Medicine (IBYME-CONICET, Argentina). Experiments were conducted in accordance with the Guide for Care and Use of Laboratory Animals published by the National Institutes of Health.

Assessment of fertility

Individual C*risp1*$^{-/-}$ males (2 to 6 months old) or their control (wild-type) littermates were housed with two females for 15 days. Mating was confirmed by the presence of vaginal plug and the fertility of

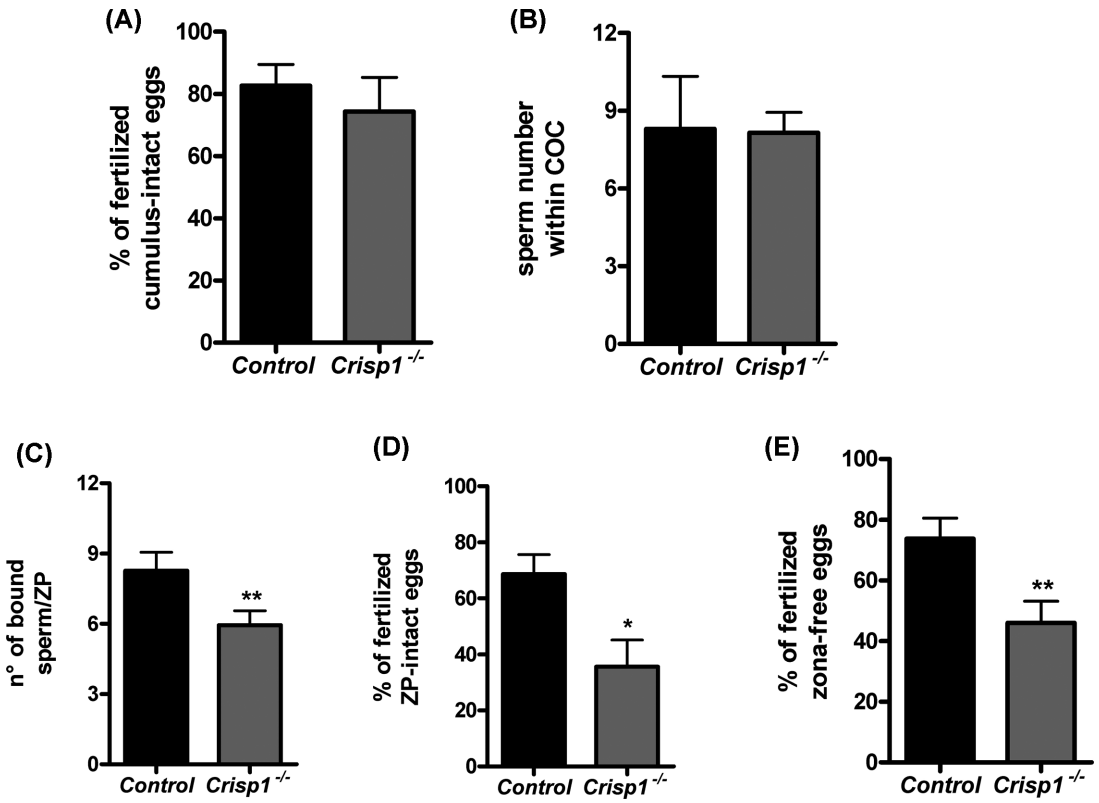

Figure 1. Behavior of CRISP1-deficient sperm at different stages of fertilization. Capacitated control or *Crisp1*$^{-/-}$ B6 sperm were co-incubated with either COC **(A)** or ZP-intact eggs **(D)** for 24 h or ZP-free eggs for 1 h **(E)**, and the percentages of fertilized eggs evaluated at the end of gamete co-incubation. Hoechst-stained capacitated sperm were co-incubated with COC for 15 min, and the number of sperm within the cumulus matrix was determined **(B)**. Capacitated sperm were co-incubated with ZP-intact eggs, and the number of sperm bound to the ZP was evaluated 30 min later **(C)**. Data are mean ± SEM, n = 5; $^{*}P < 0.05$ $^{**}P < 0.001$.

each male was analyzed and expressed as percentage of pregnant females and average litter size.

Sperm collection and in vitro capacitation

Mouse sperm were recovered by incising the cauda epididymides in 300 μl of capacitation medium [31] supplemented with 0.3% (w/v) of bovine serum albumin (BSA) (Sigma-Aldrich) under paraffin oil. Aliquots of the suspension were added to 300 μl of fresh medium previously placed in tissue culture dishes to obtain a final concentration of 0.1–1 × 10^7 cells/ml and then incubated for 90 min under paraffin oil at 37°C in an atmosphere of 5% (v/v) CO_2 in air. Alternatively, sperm were incubated for 90 min in the same medium without adding Ca^{2+} salts in the presence or absence of either EGTA (2 mM) or cyclosporin A (CSA) (10 μM). For some experiments, sperm were incubated in capacitation conditions containing either a cAMP analog, N6,2′-O-dibutyryladenosine 3′,5′-cyclic monophosphate sodium salt (dbcAMP) (5 mM) and 3-isobutyl-1-methylxanthine (IBMX) (0.2 mM), an inhibitor of the phosphodiesterase (PDE), or different concentrations of the bicarbonate ion. All the compounds used in these experiments were from Sigma.

Immunoblot analysis

Immunoblot analysis was performed as previously described [17]. Briefly, for preparation of tissue extracts, epididymides were homogenized in 50 mM Tris-HCl buffer (pH: 7.4) containing 0.2 mM phenylmethylsulphonyl fluoride (PMSF; Sigma-Aldrich). Sperm suspensions obtained before or after capacitation were washed with phosphate-buffered saline (PBS) (137mM NaCl, 10 mM Na_2HPO_4, 1.8 mM KH_2PO_4, pH: 7.4). All samples were then resuspended in Laemmli sample buffer [32]. For evaluation of PKA substrate phosphorylation (pPKAs) and pTyr, sperm extracts were then treated with 70 mM 2-mercaptoethanol (Sigma-Aldrich). Tissue (2 μg/lane) or sperm (2 × 10^6/lane) extracts were separated by SDS-PAGE and transferred onto nitrocellulose membranes. After blocking with 2% (w/v) skim milk in PBS, the membranes were probed with the primary antibody followed by exposure to the corresponding peroxidase-conjugated secondary antibody (see antibody details in Supplementary Table S1). The immunoreactive proteins were detected by an ECL Western blotting kit (GE Healthcare) and images captured with G: BOX GENI (Syngene, Synoptics Ltd) according to the manufacturer's instructions. Tubulin and Tyr phosphorylated hexokinase served as loading controls for pPKAs and pTyr blots, respectively [1, 33].

Analysis of sperm functional parameters

a) *Viability:* Ten microliters of sperm suspensions were placed on prewarmed slides and analyzed under a light microscope (×200) using Eosin Y staining (Sigma-Aldrich).

b) *Spontaneous and progesterone-induced AR:* the acrosomal status was evaluated by Coomassie Brilliant Blue staining as described elsewhere [34]. At least 400 spermatozoa were evaluated in each treatment under a light microscope (×400). Sperm were scored as acrosome-intact when a bright blue staining was observed in the dorsal region of the head or as acrosome-reacted when no

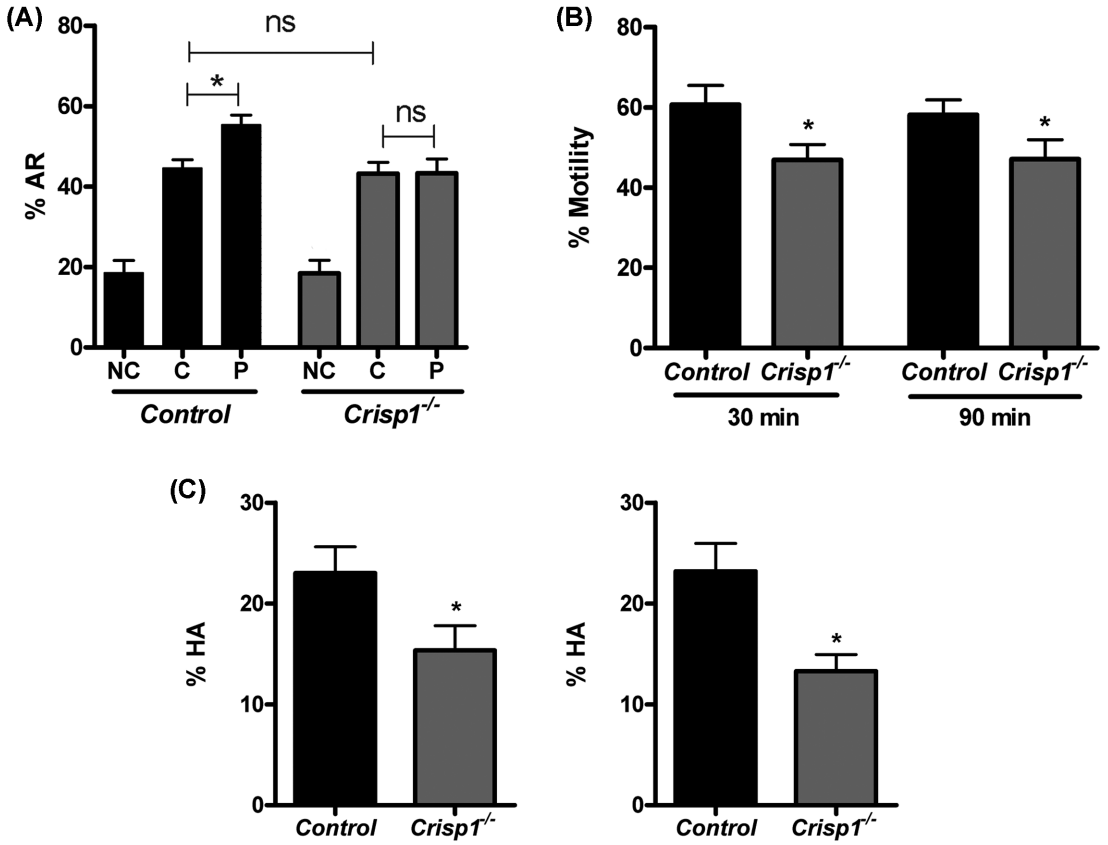

Figure 2. Capacitation-associated events in CRISP1-deficient sperm. Control and *Crisp1*$^{-/-}$ B6 sperm were incubated under capacitating conditions for up to 90 min and different functional parameters evaluated. (A) Percentage of AR determined by Coomassie Brilliant Blue staining in noncapacitated (NC) or capacitated sperm exposed to either DMSO (C) or progesterone (P). n = 6. $^*P < 0.05$; ns: non-significant. (B) Percentage of motile sperm evaluated by video microscopy at 30 and 90 min of incubation. n = 5; $^*P < 0.05$. (C) Percentage of HA evaluated by CASA at 90 min of incubation in B6 (left panel) and 129/B6 (right panel) sperm. n = 5; $^*P < 0.05$. In all cases, data are mean ± SEM.

labeling was observed. For induction of the AR, progesterone (P4; 15 μM final concentration; Sigma-Aldrich) in dimethylsulfoxide (DMSO) was added to capacitating sperm during the last 15 min of incubation.

c) *Motility:* sperm motility was analyzed by video microscopy as previously reported [34]. Ten microliters of sperm suspensions were placed on prewarmed slides and sperm movement was recorded at 30 frames/s with a Coolpix L20 camera (Nikon) in an Eclipse TS100 microscope (Nikon) using LWD 20×/0.40 Ph1 ADL ∞/1.2 WD 3.0 objective lenses. The percentage of motile sperm was calculated by analyzing a minimum of 300 cells distributed in at least 20 different microscope fields.

d) *HA:* Evaluation of sperm HA was carried out by computer-assisted sperm analysis (CASA). Sperm aliquots (15 μl) were placed between prewarmed slides and cover slips (22 × 22 mm) to create a chamber with ~30 μm depth, and were examined at 37°C using the ISAS (Integrated Semen Analysis System) v1.2 CASA system (Proiser R&D). For each sample, a minimum of 200 cells distributed in at least 20 different microscope fields were scored (30 frames acquired at 60 Hz for each measurement). The following parameters were evaluated: average path velocity (VAP, μm/s), curvilinear velocity (VCL, μm/s), straight line velocity (VSL, μm/s), linearity (LIN, %), amplitude of lateral head displacement (ALH, μm), straightness (STR, %), and beat cross frequency (BCF, Hz). Sperm were considered motile when showing VSL > 0, and hyperactivated when presenting VCL ≥ 269, LIN < 31.9%, and ALH ≥ 5.6. These custom cutoffs were selected for our experimental conditions based on previously reported recommendations [35].

Recovery and treatment of oocytes

C57BL/6 female mice (2–4 months old) were superovulated by an injection (i.p.) of equine chorionic gonadotropin (5 UI; Syntex), followed by the administration (i.p.) of human chorionic gonadotropin (hCG; 5UI; Syntex) 48 h later. Oocytes were collected from the oviducts of superovulated animals 12–13 h after hCG administration. For cumulus cells removal, the oocyte–cumulus complexes (COC) were incubated for 3 min in 0.3 mg/ml hyaluronidase (type IV; Sigma-Aldrich). The ZP was dissolved by treating the oocytes with acid Tyrode solution (pH 2.5) for 10 s [36].

In vitro fertilization assays

Intact COC or cumulus-free ZP-intact eggs were inseminated with capacitated sperm (final concentration 0.5–2 × 10^5 sperm/ml), and gametes were co-incubated in an atmosphere of 5% (v/v) CO_2 in air for 24 h at 37°C. ZP-free eggs were inseminated with capacitated sperm (final concentration: 0.5–1 × 10^4 cells/ml), and gametes were co-incubated for 1 h. At the end of incubations, eggs were washed, fixed with 2% (w/v) paraformaldehyde (PFA), stained with 1 μg/μl

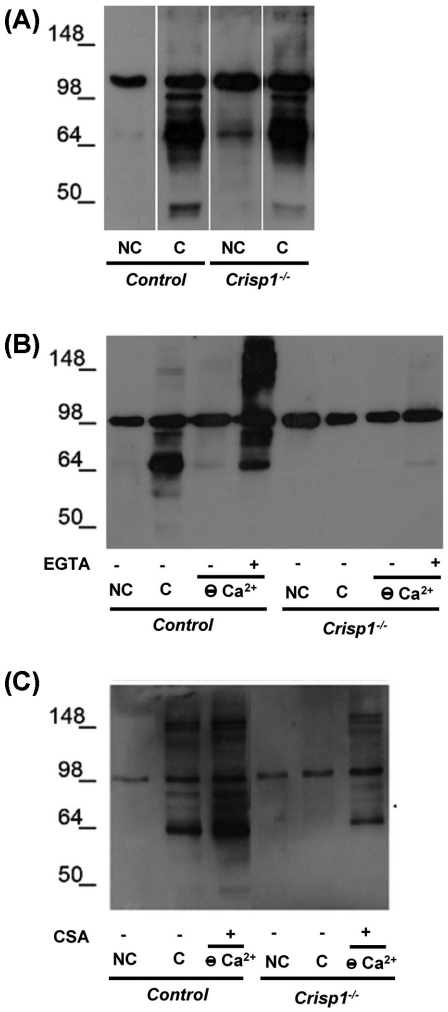

Figure 3. Protein tyrosine phosphorylation in CRISP1-deficient sperm. Protein extracts from control and *Crisp1*$^{-/-}$ sperm were incubated under different conditions and analyzed by western blotting using an anti-pTyr antibody. (A) Sperm from the B6 colony; (B and C) sperm from 129/B6 colony. NC: non-capacitated sperm; C: capacitated sperm; ⊖ Ca^{2+}: incubation medium without added Ca^{2+}. CSA: cyclosporin A. In all cases, a representative western blot from at least three different experiments is shown.

Hoechst 33342 (Sigma-Aldrich), mounted on slides, and analyzed under a Nikon Optiphot microscope (Nikon) equipped with epifluorescence optics (×200). Eggs were considered fertilized by the presence of two-cell embryos after 24-h incubation or if at least one decondensing sperm nucleus was observed after 1 h of co-incubation.

Sperm-zona pellucida binding assay

Zona pellucida-intact eggs were co-incubated with capacitated sperm (final concentration: 1 × 10^5 cells/ml) for 30 min at 37°C in an atmosphere of 5% (v/v) CO_2 in air. Eggs and embryos were washed thoroughly until no sperm remained bound to the embryos. Finally, eggs were fixed and the number of sperm bound to the ZP was counted under a light microscope (×400).

Cumulus penetration assay

COC were inseminated with capacitated sperm (final concentration: 1–2.5 × 10^4 sperm/ml) previously stained with 3 μg/ml Hoechst 33342, and gametes were co-incubated for 15 min at 37°C in an atmosphere of 5% (v/v) CO_2 in air. COC were washed and fixed with 2% (w/v) PFA, and the number of sperm within the cumulus was determined under the Nikon Optiphot microscope (Nikon) equipped with epifluorescence optics (×200).

Intracellular Ca^{2+} measurement

Intracellular Ca^{2+} levels were measured by flow cytometry as previously described [37]. Sperm aliquots were incubated in a capacitating or noncapacitating (without bicarbonate and BSA) Whitten HEPES-buffered medium [38] for 1 h and then loaded with 2 μM of Fluo-4-AM (Invitrogen) diluted in 10% (w/v) Pluronic F-127 (Invitrogen). Samples were washed to remove the excess of probe, suspended in BSA-free medium, and exposed to 2.5 μg/ml propidium iodide (PI; Sigma-Aldrich). Fluorescence was detected using a BD FACS CantoTM II (BD Biosciences) analyzer following the manufacturer's indications. Data analysis was performed by FlowJo 7.6 software (FlowJo LLC). Mean fluorescence intensity for Fluo-4 AM was obtained from at least 10 000 live (PI negative) sperm.

Intracellular cAMP measurement

Aliquots of capacitated sperm were washed twice by centrifugation and sperm pellets resuspended in 100% ethanol (Merck). Sperm suspensions were then centrifuged at 15,000 g, and the supernatants were transferred to other tubes, air dried, and then resuspended in sodium acetate buffer 50 mM, pH: 6.2. Samples were finally subjected to radioimmunoassay (RIA) as previously described [39].

cAMP phosphodiesterase assays

Spermatozoa were incubated in capacitation medium for 10 min, washed, and then treated with lysis buffer (50 mM Tris-HCl solution pH: 8, Triton X-100 1%, 14 mM β-mercaptoethanol and protease inhibitor (PMSF)) for 30 min. The suspensions were centrifuged at 13 000 g for 8 min and PDE activity was determined in the soluble fraction (supernatant) as described previously [40]. The reaction was performed by incubating the total supernatant with 20 mM Tris–HCl, pH 7.5, 5 mM Mg^{2+}, and 50 μM [3H] cAMP for 20 min at 30°C.

Statistical analysis

Data represent the mean ± SEM from at least three independent experiments. Calculations were performed using the Prism 5.0 software (GraphPad Software). In all cases, comparisons were made by the Student *t*-test and differences were considered significant at a level of $P < 0.05$.

Results

CRISP1-deficient mice originally generated in a mixed 129/SvEv∗C57BL/6 background (129/B6) [17] were backcrossed to the C57BL/6 (B6) strain to reach at least 99.95% level of homogeneity. Western blot studies confirmed the lack of the target protein in epididymal tissue and sperm extracts from B6 *Crisp1*$^{-/-}$ mice and revealed normal expression of CRISP4, the other epididymal member of the CRISP protein family (Supplementary Figure S1).

To study the fertility of males from the B6 colony, each *Crisp1*$^{-/-}$ or control male was caged with two control females during 15 days as previously reported for the 129/B6 colony [17]. Under these conditions, no differences were observed in either the percentage of pregnant females or average litter size corresponding to *Crisp1*$^{-/-}$ animals compared to controls (Table 1). The next step was to

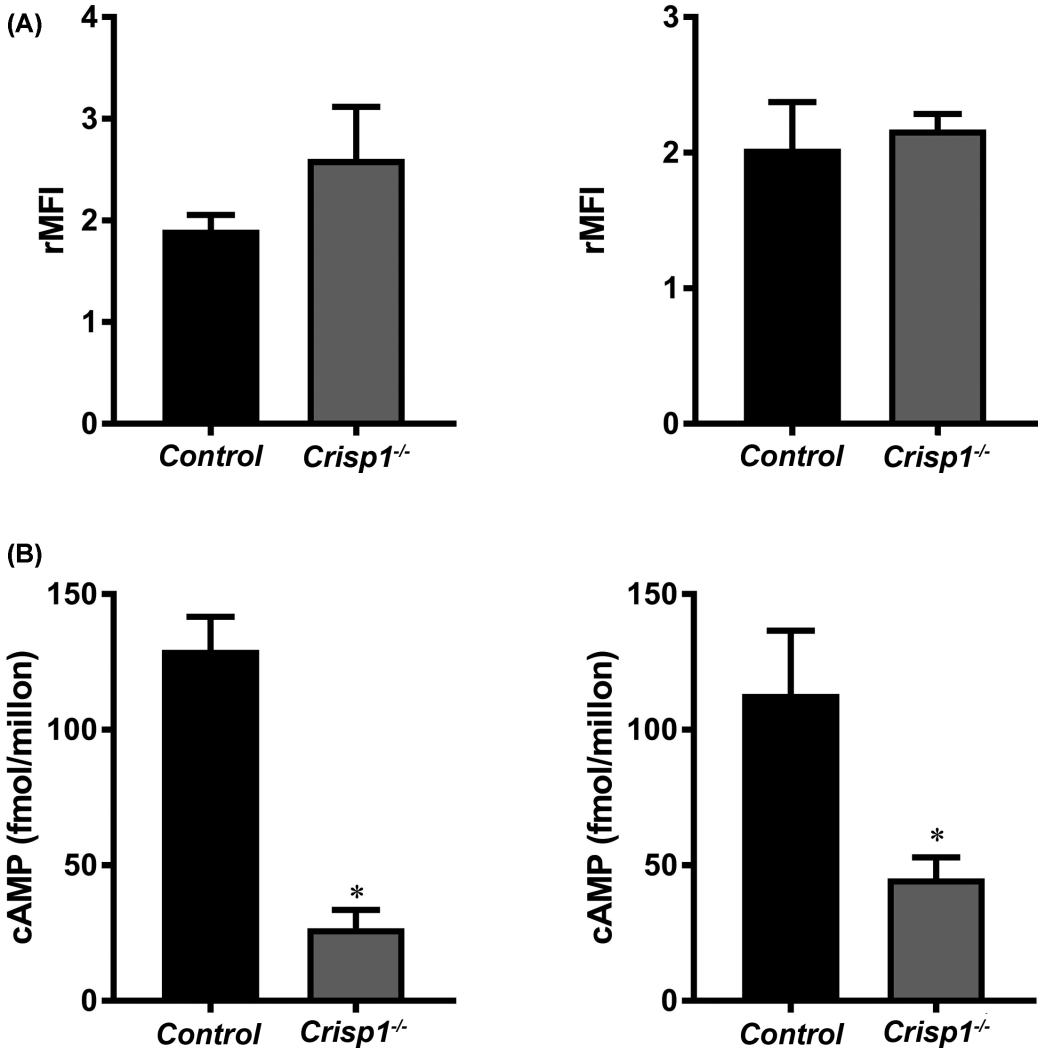

Figure 4. Secondary messengers in CRISP1-deficient sperm. (A) Control and *Crisp1*$^{-/-}$ sperm incubated under capacitating conditions for 90 min were exposed to Fluo-4 AM and intracellular Ca^{2+} levels of viable sperm were measured by flow cytometry. Results are shown as relative mean fluorescence intensity (rMFI) between capacitated and noncapacitated sperm. Results represent the mean ± SEM of at least three experiments; ns. (B) Control and *Crisp1*$^{-/-}$ sperm were incubated under capacitating conditions for 30 min, and cAMP levels were determined by RIA. Results represent the mean ± SEM. n = 5; $^{*}P < 0.05$. (A and B): left panel: B6 mice; right panel: 129/B6 mice.

analyze different sperm functional parameters in B6 mutant spermatozoa. No significant differences compared to controls were observed in either sperm number (control 30 ± 5 millions vs *Crisp1*$^{-/-}$ 25 ± 6 millions, n = 6, ns) or sperm viability (control 50 ± 4% vs *Crisp1*$^{-/-}$ 46 ± 2%, n = 6, ns). Then, we analyzed the fertilizing ability of capacitated *Crisp1*$^{-/-}$ and control spermatozoa from B6 mice by *in vitro* fertilization using either COC, ZP-intact, or ZP-free eggs. As previously reported for the mixed 129/B6 background [17, 18, 41] whereas no differences in the percentage of fertilized eggs or in the number of sperm penetrating the cumulus were observed for *Crisp1*$^{-/-}$ or control sperm exposed to control COC (Figure 1A and B), *Crisp1*$^{-/-}$ spermatozoa exhibited significant deficiencies to bind to the ZP and to fertilize both ZP-intact and ZP-free eggs compared to controls (Figure 1C–E). Further characterization of sperm functional parameters revealed that capacitated B6 *Crisp1*$^{-/-}$ sperm showed normal spontaneous AR but a deficiency to acrosome-react in response to progesterone (Figure 2A) not previously observed for 129/B6 sperm [17]. In addition, our studies revealed a significant reduction in total motility of B6 *Crisp1*$^{-/-}$ sperm incubated under capacitating conditions (Figure 2B) not observed for mutant sperm of the mixed background [17] as well as significantly lower percentages of HA compared to controls in *Crisp1*$^{-/-}$ sperm from both colonies (Figure 2C, Supplementary Table S2). Interestingly, B6 *Crisp1*$^{-/-}$ spermatozoa exhibited normal levels of pTyr (Figure 3A) in contrast to the marked reduction in pTyr reported for null spermatozoa from the mixed background [17]. To explore the mechanisms leading to the pTyr decrease observed in 129/B6 *Crisp1*$^{-/-}$ sperm, these cells were subjected to two approaches known to increase pTyr [42], i.e., incubation in a medium lacking added Ca^{2+} and containing either EGTA to chelate residual Ca^{2+}or CSA, an inhibitor of the Ca^{2+}-dependent Ser/Thr phosphatase calcineurin [42, 43]. Results showed that whereas the pTyr deficiency of *Crisp1*$^{-/-}$ sperm was refractory to exposure to EGTA (Figure 3B, lane 4 vs lane 8), it could be overcome by exposing the cells to CSA (Figure 3C, lane 3 vs lane 6).

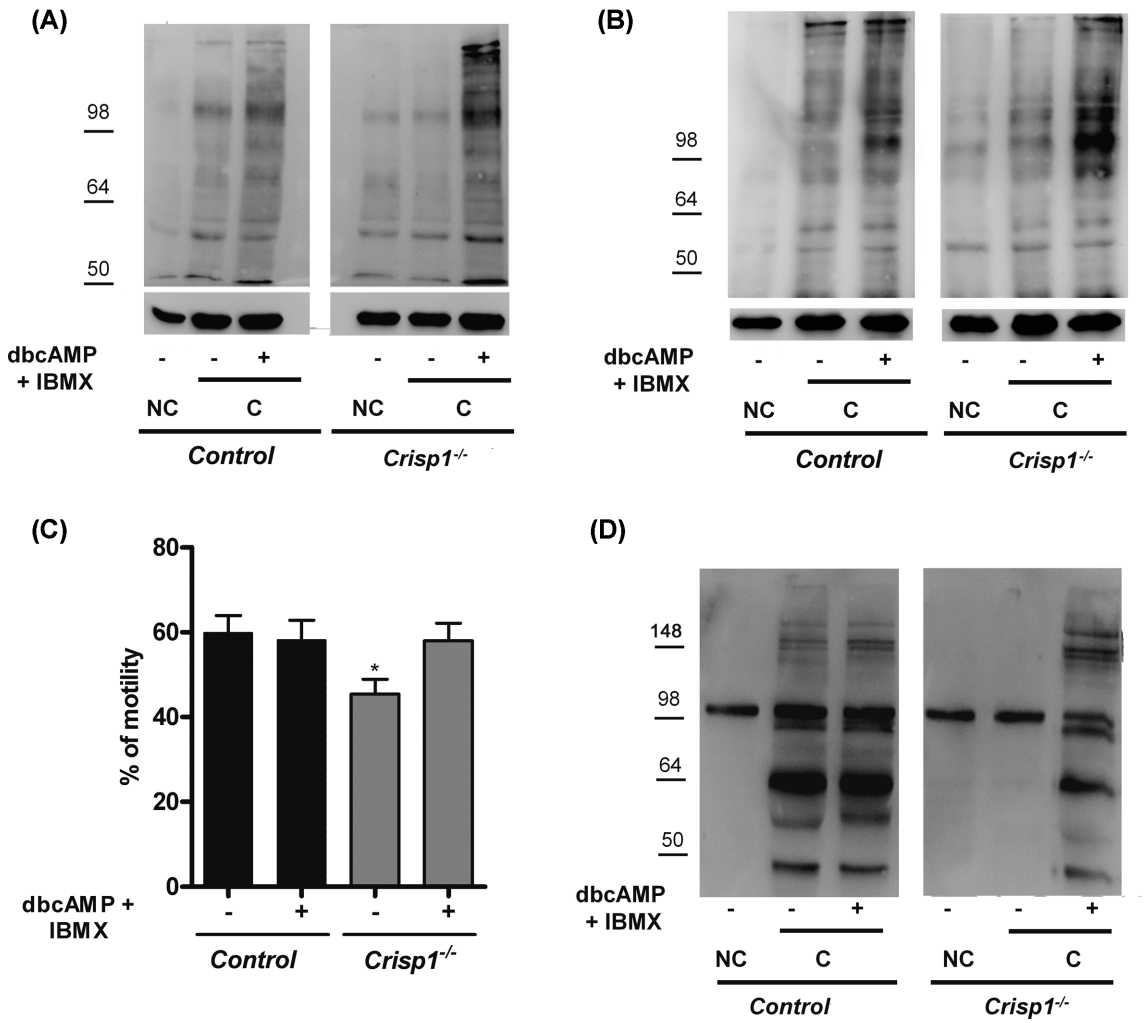

Figure 5. Rescue of functional deficiencies in CRISP1-deficient sperm. Control and *Crisp1*$^{-/-}$ sperm were exposed to dbcAMP and IBMX during capacitation and different parameters were evaluated. (A, B) Protein extracts from B6 (A) or 129/B6 (B) sperm were analyzed for pPKAs by western blotting using an anti-pPKAs antibody (top). Anti-tubulin antibody was used as loading control (bottom). (C) The percentage of sperm motility was determined by video microscopy in B6 sperm at 30 min of incubation in a capacitating medium. Results represent the mean ± SEM. n = 7; $^{*}P < 0.05$. (D) Protein extracts were analyzed for pTyr by western blotting with an anti-pTyr antibody in 129/B6 sperm. In all cases, a representative western blot from at least three different experiments is shown. NC: non-capacitated sperm. C: capacitated sperm.

The above observations suggest a deregulation of the signaling cascades involving Ca^{2+} and/or cAMP, two key regulators of capacitation-associated events [44, 45]. Based on this, intracellular levels of these molecules were analyzed in spermatozoa from both colonies incubated under capacitating conditions. Flow cytometry studies were unable to detect significant differences in intracellular Ca^{2+} levels as a consequence of capacitation between *Crisp1*$^{-/-}$ and control spermatozoa from either colony (Figure 4A). Evaluation of cAMP by RIA, on the other hand, detected significantly lower levels of this messenger at the beginning of the incubation in null spermatozoa from both genetic backgrounds compared to controls (Figure 4B). To explore whether these lower cAMP levels were due to a higher hydrolysis of the molecule, PDE levels in sperm were analyzed observing no significant differences between mutant and control cells in either colony (Supplementary Figure S2).

Consistent with the lower levels of cAMP, capacitated *Crisp1*$^{-/-}$ sperm from both colonies exhibited defects in pPKAs that could be reverted by exposure of sperm to dbcAMP (a cAMP agonist) plus IBMX (a PDE inhibitor) during capacitation (Figure 5A and B) but not by exposing sperm to higher concentrations of bicarbonate, a stimulator of soluble adenylyl cyclase (SACY) [46] (Supplementary Figure S3). Moreover, incubation of sperm with dbcAMP plus IBMX was capable of recovering the reduced motility and pTyr levels of B6 and 129/B6 spermatozoa, respectively (Figure 5C and D), indicating that a cAMP/PKA signaling defect common to both colonies led to different phenotypes depending on the genetic background of the animals.

Discussion

In the present work, we explored the influence of the genetic background on the reproductive phenotype produced by a mutation in the *Crisp1* gene. As previously reported for the mixed 129/B6 colony [17], the lack of CRISP1 did not affect the fertility of males from the homogeneous B6 colony indicating that fertility is not influenced by a change in the genetic background at least when analyzed under

Table 2. Comparison of functional phenotypes between the two colonies.

		129/B6 *Crisp1*$^{-/-}$	B6 *Crisp1*$^{-/-}$
Fertility		Normal	Normal
Fertilizing ability	**COC-intact eggs**	Normal	Normal
	ZP-intact eggs	Decreased (38%)	Decreased (48%)
	ZP-free eggs	Decreased (33%)	Decreased (38%)
	Cumulus penetration	Normal	Normal
	ZP Binding	Decreased (28%)	Decreased (29%)
P4-induced AR		Normal	Decreased
pPKAs		Decreased	Decreased
pTyr		Decreased	Normal
Motility		Normal	Decreased
Hyperactivation		Decreased	Decreased

% of inhibition is indicated between brackets.

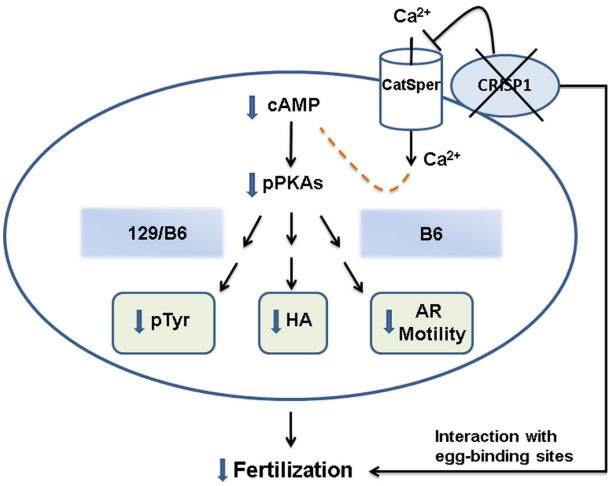

Figure 6. Influence of the genetic background on functional defects of CRISP1-deficient sperm. *Crisp1*$^{-/-}$ sperm from 129/B6 and B6 genetic backgrounds exhibit common defects in the cAMP-PKA signaling cascade that lead to HA defects in both colonies and to lower levels of pTyr, motility, or progesterone-induced AR depending on the genetic background of the animal. Capacitation-associated defects together with the lack of interaction between CRISP1 and its egg-binding sites contribute to the impaired fertilization observed in mutant sperm from both colonies.

ideal laboratory breeding conditions. It is important to note, however, that the CRISP family members exhibit a high sequence and functional homology [5], supporting the existence of a functional compensation among these proteins. Considering that CRISP4-null mice of different genetic backgrounds are also fertile [47, 48], it is possible that these compensatory mechanisms are responsible for the lack of fertility defects observed in CRISP KO mice from even different genetic backgrounds. This hypothesis is currently under investigation in our laboratory.

In spite of their normal fertility, *Crisp1*$^{-/-}$ males from the B6 colony showed spermatozoa with impaired ability to fertilize both ZP-intact and ZP-free eggs, supporting the proposed role of CRISP1 in both sperm–ZP interaction and gamete fusion [14, 15, 17]. Although the lower fertilization rates of ZP-intact eggs can be attributed to the lower levels of sperm-ZP binding, we cannot exclude the possibility that sperm also exhibit defects at the ZP-penetration step itself which are difficult to analyze due to the previous impaired sperm-ZP binding. Supporting a possible defect at the ZP-penetration level, sperm from both colonies exhibit clear deficiencies to develop HA, which is essential for ZP penetration and proposed to be modulated by the ability of CRISP1 to regulate CatSper [18]. Considering the absolute need of the AR for both penetration of the ZP and gamete fusion, the lower levels of induced-AR observed in B6 *Crisp1*$^{-/-}$ sperm might have impact on these two stages of the fertilization process. Moreover, in view of recent observations showing that mouse sperm undergo the AR prior to reaching the COC in the ampulla [49–51], it is possible that the AR is also beneficial or even required for successful cumulus penetration. However, as summarized in Table 2, cumulus penetration was not affected in either background whereas gamete fusion was similarly reduced in both colonies and evaluated using ZP-free eggs which allows the analysis of the spontaneous rather than the induced AR. The fertilization deficiencies observed using cumulus-free eggs were not detected when B6 null sperm were exposed to COC. Given the reported relevance of cumulus CRISP1 for fertilization [18], it is likely that the beneficial effects of the cumulus [52] and CRISP1 within the COC compensate the deficiencies of *Crisp1*$^{-/-}$ spermatozoa in both genetic backgrounds.

Whereas the analysis of fertilization results revealed that CRISP1 mutant sperm from the B6 background showed defects at the same fertilization stages and at similar levels than those reported for 129/B6 mice (see Table 2), several sperm functional parameters such as progesterone-induced AR, motility, and pTyr showed a clear dependence on the genetic background of the animals. Considering the relevance of these functional events for the sperm fertilizing ability, it is possible they contribute differently in each background leading to the similar fertilization rates observed. In addition, fertilization defects might well be explained by the lack of interaction between CRISP1 and its egg-complementary sites (see Figure 6).

To gain insights into the molecular mechanisms underlying the functional defects observed in *Crisp1*$^{-/-}$ mice, we next analyzed possible alterations in the levels of key regulators of capacitation-associated events. The observation that 129/B6 *Crisp1*$^{-/-}$ sperm incubated in a medium lacking Ca^{2+} did not show the expected increase in pTyr when exposed to EGTA [42] but did so when exposed to a calcineurin inhibitor supports the existence of a deregulation in intracellular Ca^{2+} and/or cAMP levels in these cells. Analysis of cAMP revealed significantly lower levels of this important messenger in mutant compared to control sperm in both colonies, a defect that could not be attributed to a higher hydrolysis of the molecule according to sperm PDE activity assays. Consistent with the lower cAMP content, *Crisp1*$^{-/-}$ sperm exhibited lower pPKAs levels which could not be overcome by exposure of the cells to higher concentrations of bicarbonate, suggesting that the lack of CRISP1 might be affecting either SACY activity *per se* and/or other associated events (i.e. changes at the plasma membrane that affect bicarbonate influx, changes in Ca^{2+} concentrations required for SACY activation, lower ATP levels, higher cAMP extrusion, etc.). Interestingly, while there is usually a positive correlation between pPKAs and pTyr, our results show that the decrease in pPKAs can be accompanied by either reduced or normal pTyr levels depending on the genetic background. In agreement with this, it has been reported that sperm lacking epididymal ribonuclease Rnase 9 also exhibit a decrease in pPKAs and normal levels of pTyr [53].

Evaluation of intracellular Ca^{2+} by flow cytometry studies failed to detect significant changes compared to controls in *Crisp1*$^{-/-}$ sperm from both backgrounds. However, given the reported ability of CRISP1 to affect both CatSper currents and intracellular Ca^{2+}

levels [18], it is possible to hypothesize that the lack of CRISP1 in mutant sperm produces a Ca^{2+} deregulation which is compensated by other mechanisms and, thus, not reflected in the total concentration of the cation within the cell. Moreover, considering the cross-talk between Ca^{2+} and cAMP signaling pathways [42], it is possible that an intracellular Ca^{2+} deregulation leads to the low levels of cAMP observed in *Crisp1*$^{-/-}$ sperm from both backgrounds. Of note in this regard, CatSper has been proposed to be involved in the initial cross-talk between Ca^{2+} and cAMP-dependent cascades and *CatSper*$^{-/-}$ sperm show increases in cAMP and pPKAs levels [54, 55] that are consistent with the reduction in these two parameters observed in *Crisp1*$^{-/-}$ sperm from both colonies.

The observation that dbcAMP and IBMX restored pPKAs in both colonies as well as pTyr and motility levels in 129/B6 and B6 C*risp1*$^{-/-}$ sperm, respectively, suggests that mutant sperm from both genetic backgrounds exhibit a common defect in the cAMP-PKA signaling cascade that leads to different phenotypes depending on the genetic background of the animal (Figure 6). Although the molecular mechanisms underlying the different phenotypes remain to be elucidated, it is known that phenotypes are rarely an intrinsic property of target alleles but instead result from integration of their activities with environmental context and genetic background [23, 56, 57]. In our study, as mice from the two different genetic backgrounds exhibited the same mutation (i.e. lack of *Crisp1* gene) and were evaluated under the same environmental conditions, the effects of genetic modifiers acting in combination with CRISP1 at genomic, transcriptomic, or proteomic level are the most likely explanation for the phenotypic differences observed between the two colonies. Thus, considering the common cAMP defect observed in sperm from both backgrounds, it is possible that the genetic context has a different impact on the levels or functionality of the downstream proteins proposed to be involved in the AR (i.e. EPAC, Rho GTPases) [58, 59], motility (i.e. RAPGEFs) [60], or pTyr (PYK2, Fer-T) [61, 62], and/or of other molecules not yet identified. Moreover, considering that cAMP as well as several other signaling molecules (i.e. SACY, PDE, PKA, etc.) localize in discrete microdomains within the cell, playing different roles [63–67], it is also possible that modifier genes differently affect these functional compartments leading to the different phenotypes observed in the sperm head (AR) and tail (motility, pTyr). In this sense, the study of C*risp1*$^{-/-}$ mice from different backgrounds may represent an interesting model to identify the yet unknown molecules involved in the signaling cascade leading to capacitation.

Altogether, our findings indicate that the phenotype observed in CRISP1 null males is not entirely controlled by the mutation at *Crisp1* locus but it is modulated by the genetic context. Interestingly, our studies reveal new roles for CRISP1 in functional events associated to capacitation (i.e. AR, motility, HA) as well as in the cAMP-PKA signaling cascade underlying this process. Whereas the defects in fertilization, HA, and cAMP/PKA signaling pathway of CRISP1 mutant sperm seem to withstand the different genetic contexts, progesterone-induced AR, motility, and pTyr defects were clearly dependent on the genetic background of the animals (Figure 6). These observations may reflect the human situation where patients with the same disease-causing mutation often show phenotypic variations due to the genetic heterogeneity inherent to individuals [23, 56, 57]. Thus, the analysis of the reproductive phenotypes associated with a single mutation in different genetic backgrounds may contribute to identify those traits that are better candidate targets for treatment of infertility and/or contraceptive development.

Supplementary data

Supplementary data are available at *BIOLRE* online.

Supplementary Figure S1. Expression of CRISP1 and CRISP4 in CRISP1-deficient mice. Protein extracts obtained from the epididymis and spermatozoa from control or C*risp1*$^{-/-}$ B6 mice were subjected to SDS-PAGE and western blotting using anti-CRISP1 and anti-CRISP4 primary antibodies. Identical results were obtained for the mixed 129/B6 colony.

Supplementary Figure S2. Phosphodiesterase (PDE) activity in CRISP1-deficient sperm. PDE activity was determined in the soluble fraction (supernatant) of lysed spermatozoa that were previously incubated under capacitating conditions for 10 min. (A) sperm from the B6 colony; (B) sperm from 129/B6 colony.

Supplementary Figure S3. Effect of HCO_3^- concentration on pPKAs in CRISP1-deficient sperm. Protein extracts from B6 (A) or 129/B6 (B) sperm were incubated for 90 min under capacitating conditions in the presence of increasing bicarbonate concentrations (from 0 to 50 mM) and analyzed for pPKAs by western blotting using an anti-pPKAs antibody. Anti-tubulin antibody was used as loading control. A representative western blot from at least three different experiments is shown.

Supplementary Table S1. Antibodies used.

Supplementary Table S2. Sperm motility parameters evaluated by CASA.

Acknowledgments

The authors thank Pereyra E and Dr Schoijet A for their technical help in cAMP and PDE determinations, respectively, the Semen Quality and Cryopreservation unit at INITRA (Facultad de Ciencias Veterinarias, UBA) for the CASA installations and Dr Rubinstein M, Dr Alonso G, and members of Dr Cuasnicú laboratory for their helpful comments.

References

1. Visconti PE, Bailey JL, Moore GD, Pan D, Olds-Clarke P, Kopf GS. Capacitation of mouse spermatozoa. I. Correlation between the capacitation state and protein tyrosine phosphorylation. *Development* 1995; **121**:1129–1137.
2. Visconti PE, Moore GD, Bailey JL, Leclerc P, Connors SA, Pan D, Olds-Clarke P, Kopf GS. Capacitation of mouse spermatozoa. II. Protein tyrosine phosphorylation and capacitation are regulated by a cAMP-dependent pathway. *Development* 1995; **121**:1139–1150.
3. Ruknudin A, Silver IA. Ca2+ uptake during capacitation of mouse spermatozoa and the effect of an anion transport inhibitor on Ca2+ uptake. *Mol Reprod Dev* 1990; **26**:63–68.
4. Da Ros VG, Muñoz MW, Battistone MA, Brukman NG, Carvajal G, Curci L, Gómez-Elías MD, Cohen DBJ, Cuasnicu PS. From the epididymis to the egg: participation of CRISP proteins in mammalian fertilization. *Asian J Androl* 2015; **17**:711–715.
5. Gibbs GM, Roelants K, O'Bryan MK. The CAP superfamily: cysteine-rich secretory proteins, antigen 5, and pathogenesis-related 1 proteins—roles in reproduction, cancer, and immune defense. *Endocr Rev* 2008; **29**:865–897.
6. Guo M, Teng M, Niu L, Liu Q, Huang Q, Hao Q. Crystal structure of the cysteine-rich secretory protein stecrisp reveals that the cysteine-rich domain has a K+ channel inhibitor-like fold. *J Biol Chem* 2005; **280**:12405–12412.
7. Gibbs GM, Scanlon MJ, Swarbrick J, Curtis S, Gallant E, Dulhunty AF, O'Bryan MK. The cysteine-rich secretory protein domain of Tpx-1 is related to ion channel toxins and regulates ryanodine receptor Ca^{2+} signaling. *J Biol Chem* 2006; **281**:4156–4163.

8. Cameo MS, Blaquier JA. Androgen-controlled specific proteins in rat epididymis. *J Endocrinol* 1976; **69**:47–55.
9. Garberi JC, Kohane AC, Cameo MS, Blaquier JA. Isolation and characterization of specific rat epididymal proteins. *Mol Cell Endocrinol* 1979; **13**:73–82.
10. Garberi JC, Fontana JD, Blaquier JA. Carbohydrate composition of specific rat epididymal protein. *Int J Androl* 1982; **5**:619–626.
11. Kohane AC, González Echeverría FM, Piñeiro L, Blaquier JA. Interaction of proteins of epididymal origin with spermatozoa. *Biol Reprod* 1980; **23**:737–742.
12. Cohen DJ, Rochwerger L, Ellerman DA, Morgenfeld MM, Busso D, Cuasnicú PS. Relationship between the association of rat epididymal protein "DE" with spermatozoa and the behavior and function of the protein. *Mol Reprod Dev* 2000; **56**:180–188.
13. Roberts KP, Wamstad JA, Ensrud KM, Hamilton DW. Inhibition of capacitation-associated tyrosine phosphorylation signaling in rat sperm by epididymal protein Crisp-1. *Biol Reprod* 2003; **69**:572–581.
14. Busso D, Cohen DJ, Maldera JA, Dematteis A, Cuasnicu PS. A novel function for CRISP1 in rodent fertilization: involvement in sperm-zona pellucida interaction. *Biol Reprod* 2007; **77**:848–854.
15. Cohen DJ, Ellerman DA, Cuasnicú PS. Mammalian sperm-egg fusion: evidence that epididymal protein DE plays a role in mouse gamete fusion. *Biol Reprod* 2000; **63**:462–468.
16. Rochwerger L, Cohen DJ, Cuasnicú PS. Mammalian sperm-egg fusion: the rat egg has complementary sites for a sperm protein that mediates gamete fusion. *Dev Biol* 1992; **153**:83–90.
17. Da Ros VG, Maldera JA, Willis WD, Cohen DJ, Goulding EH, Gelman DM, Rubinstein M, Eddy EM, Cuasnicu PS. Impaired sperm fertilizing ability in mice lacking Cysteine-RIch Secretory Protein 1 (CRISP1). *Dev Biol* 2008; **320**:12–18.
18. Ernesto JI, Weigel Muñoz M, Battistone MA, Vasen G, Martínez-López P, Orta G, Figueiras-Fierro D, De la Vega-Beltran JL, Moreno IA, Guidobaldi HA, Giojalas L, Darszon A et al. CRISP1 as a novel CatSper regulator that modulates sperm motility and orientation during fertilization. *J Cell Biol* 2015; **210**:1213–1224.
19. Ren D, Navarro B, Perez G, Jackson AC, Hsu S, Shi Q, Tilly JL, Clapham DE. A sperm ion channel required for sperm motility and male fertility. *Nature* 2001; **413**:603–609.
20. Brenker C, Goodwin N, Weyand I, Kashikar ND, Naruse M, Krahling M, Muller A, Kaupp UB, Strunker T. The CatSper channel: a polymodal chemosensor in human sperm. *EMBO J* 2012; **31**:1654–1665.
21. Smith JF, Syritsyna O, Fellous M, Serres C, Mannowetz N, Kirichok Y, Lishko PV. Disruption of the principal, progesterone-activated sperm Ca2+ channel in a CatSper2-deficient infertile patient. *Proc Natl Acad Sci USA* 2013; **110**:6823–6828.
22. Okabe M. Mechanisms of fertilization elucidated by gene-manipulated animals. *Asian J Androl* 2015; **17**:646.
23. Montagutelli X. Effect of the genetic background on the phenotype of mouse mutations. *J Am Soc Nephrol* 2000; **11 Suppl 1**:S101–S105.
24. Erickson RP. Mouse models of human genetic disease: which mouse is more like a man? *Bioessays* 1996; **18**:993–998.
25. Rozmahel R, Wilschanski M, Matin A, Plyte S, Oliver M, Auerbach W, Moore A, Forstner J, Durie P, Nadeau J, Bear C, Tsui LC. Modulation of disease severity in cystic fibrosis transmembrane conductance regulator deficient mice by a secondary genetic factor. *Nat Genet* 1996; **12**:280–287.
26. Rubinstein E, Ziyyat A, Prenant M, Wrobel E, Wolf JP, Levy S, Le Naour F, Boucheix C. Reduced fertility of female mice lacking CD81. *Dev Biol* 2006; **290**:351–358.
27. Maecker HT, Levy S. Normal lymphocyte development but delayed humoral immune response in CD81-null mice. *J Exp Med* 1997; **185**:1505–1510.
28. Nayernia K, Adham IM, Burkhardt-Göttges E, Neesen J, Rieche M, Wolf S, Sancken U, Kleene K, Engel W. Asthenozoospermia in mice with targeted deletion of the sperm mitochondrion-associated cysteine-rich protein (Smcp) gene. *Mol Cell Biol* 2002; **22**:3046–3052.
29. Odet F, Gabel S, London RE, Goldberg E, Eddy EM. Glycolysis and mitochondrial respiration in mouse LDHC-null sperm. *Biol Reprod* 2013; **88**:95.
30. Carlson AE, Westenbroek RE, Quill T, Ren D, Clapham DE, Hille B, Garbers DL, Babcock DF. CatSper1 required for evoked Ca^{2+} entry and control of flagellar function in sperm. *Proc Natl Acad Sci USA* 2003; **100**:14864–14868.
31. Fraser LR, Drury LM. The relationship between sperm concentration and fertilization in vitro of mouse eggs. *Biol Reprod* 1975; **13**:513–518.
32. Laemmli UK. Cleavage of structural proteins during the assembly of the head of bacteriophage T4. *Nature* 1970; **227**:680–685.
33. Porambo JR, Salicioni AM, Visconti PE, Platt MD. Sperm phosphoproteomics: historical perspectives and current methodologies. *Expert Rev Proteomics* 2012; **9**:533–548.
34. Vasen G, Battistone MA, Croci DO, Brukman NG, Weigel Muñoz M, Stupirski JC, Rabinovich GA, Cuasnicú PS. The galectin-1–glycan axis controls sperm fertilizing capacity by regulating sperm motility and membrane hyperpolarization. *FASEB J* 2015; **29**:4189–4200.
35. Bray C, Son J-H, Kumar P, Meizel S. Mice deficient in CHRNA7, a subunit of the nicotinic acetylcholine receptor, produce sperm with impaired motility. *Biol Reprod* 2005; **73**:807–814.
36. Nicolson GL, Yanagimachi R, Yanagimachi H. Ultrastructural localization of lectin-binding sites on the zonae pellucidae and plasma membranes of mammalian eggs. *J Cell Biol* 1975; **66**:263–274.
37. Brukman NG, Miyata H, Torres P, Lombardo D, Caramelo JJ, Ikawa M, Da Ros VG, Cuasnicú PS. Fertilization defects in sperm from Cysteine-rich secretory protein 2 (Crisp2) knockout mice: implications for fertility disorders. *Mol Hum Reprod* 2016; **22**:240–251.
38. Moore GD, Ayabe T, Visconti PE, Schultz RM, Kopf GS. Roles of heterotrimeric and monomeric G proteins in sperm-induced activation of mouse eggs. *Development* 1994; **120**:3313–3323.
39. Del Punta K, Charreau EH, Pignataro OP. Nitric oxide inhibits Leydig cell steroidogenesis. *Endocrinology* 1996; **137**:5337–5343.
40. Alonso GD, Schoijet AC, Torres HN, Flawiá MM. TcrPDEA1, a cAMP-specific phosphodiesterase with atypical pharmacological properties from *Trypanosoma cruzi*. *Mol Biochem Parasitol* 2007; **152**:72–79.
41. Cohen DJ, Maldera JA, Vasen G, Ernesto JI, Muñoz MW, Battistone MA, Cuasnicú PS. Epididymal protein CRISP1 plays different roles during the fertilization process. *J Androl* 2011; **32**:672–678.
42. Navarrete FA, García-Vázquez FA, Alvau A, Escoffier J, Krapf D, Sánchez-Cárdenas C, Salicioni AM, Darszon A, Visconti PE. Biphasic role of calcium in mouse sperm capacitation signaling pathways. *J Cell Physiol* 2015; **230**:1758–1769.
43. Miyata H, Satouh Y, Mashiko D, Muto M, Nozawa K, Shiba K, Fujihara Y, Isotani A, Inaba K, Ikawa M. Sperm calcineurin inhibition prevents mouse fertility with implications for male contraceptive. *Science* 2015; **350**:442–445.
44. Visconti PE, Krapf D, de la Vega-Beltrán JL, Acevedo JJ, Darszon A. Ion channels, phosphorylation and mammalian sperm capacitation. *Asian J Androl* 2011; **13**:395–405.
45. Buffone MG, Wertheimer EV, Visconti PE, Krapf D. Central role of soluble adenylyl cyclase and cAMP in sperm physiology. *Biochim Biophys Acta* 2014; **1842**:2610–2620.
46. Chen Y, Cann MJ, Litvin TN, Iourgenko V, Sinclair ML, Levin LR, Buck J. Soluble adenylyl cyclase as an evolutionarily conserved bicarbonate sensor. *Science (80-)* 2000; **289**:625–628.
47. Gibbs GM, Orta G, Reddy T, Koppers AJ, Martínez-López P, de la Vega-Beltràn JL, Lo JCY, Veldhuis N, Jamsai D, McIntyre P, Darszon A, O'Bryan MK. Cysteine-rich secretory protein 4 is an inhibitor of transient receptor potential M8 with a role in establishing sperm function. *Proc Natl Acad Sci USA* 2011; **108**:7034–7039.
48. Turunen HT, Sipila P, Krutskikh A, Toivanen J, Mankonen H, Hamalainen V, Bjorkgren I, Huhtaniemi I, Poutanen M. Loss of cysteine-rich secretory protein 4 (Crisp4) leads to deficiency in sperm-zona pellucida interaction in mice. *Biol Reprod* 2012; **86**:1–8.

49. Muro Y, Hasuwa H, Isotani A, Miyata H, Yamagata K, Ikawa M, Yanagimachi R, Okabe M. Behavior of mouse spermatozoa in the female reproductive tract from soon after mating to the beginning of fertilization. *Biol Reprod* 2016; **94**:80.
50. La Spina FA, Puga Molina LC, Romarowski A, Vitale AM, Falzone TL, Krapf D, Hirohashi N, Buffone MG. Mouse sperm begin to undergo acrosomal exocytosis in the upper isthmus of the oviduct. *Dev Biol* 2016; **411**:172–182.
51. Hino T, Muro Y, Tamura-Nakano M, Okabe M, Tateno H, Yanagimachi R. The behavior and acrosomal status of mouse spermatozoa in vitro, and within the oviduct during fertilization after natural mating. *Biol Reprod* 2016; **95**:50–50.
52. Yanagimachi R. Mammalian Fertilization. In: Knobil E, Neill JD (eds.), *The Physiology of Reproduction*. NY, USA: Raven Press. 1994:189–317.
53. Westmuckett AD, Nguyen EB, Herlea-Pana OM, Alvau A, Salicioni AM, Moore KL. Impaired sperm maturation in Rnase9 knockout mice. *Biol Reprod* 2014; **90**:120.
54. Carlson AE, Quill TA, Westenbroek RE, Schuh SM, Hille B, Babcock DF. Identical phenotypes of CatSper1 and CatSper2 null sperm. *J Biol Chem* 2005; **280**:32238–32244.
55. Chung J-J, Shim S-H, Everley RA, Gygi SP, Zhuang X, Clapham DE. Structurally distinct Ca^{2+} signaling domains of sperm flagella orchestrate tyrosine phosphorylation and motility. *Cell* 2014; **157**:808–822.
56. Gallati S. Disease-modifying genes and monogenic disorders: experience in cystic fibrosis. *Appl Clin Genet* 2014; **7**:133–146.
57. Riordan JD, Nadeau JH. From peas to disease: modifier genes, network resilience, and the genetics of health. *Am J Hum Genet* 2017; **101**:177–191.
58. Branham MT, Mayorga LS, Tomes CN. Calcium-induced acrosomal exocytosis requires cAMP acting through a protein kinase A-independent, Epac-mediated pathway. *J Biol Chem* 2006; **281**:8656–8666.
59. Romarowski A, Battistone MA, La Spina FA, Puga Molina L, del C, Luque GM, Vitale AM, Cuasnicu PS, Visconti PE, Krapf D, Buffone MG. PKA-dependent phosphorylation of LIMK1 and Cofilin is essential for mouse sperm acrosomal exocytosis. *Dev Biol* 2015; **405**:237–249.
60. Vadnais ML, Aghajanian HK, Lin A, Gerton GL. Signaling in sperm: toward a molecular understanding of the acquisition of sperm motility in the mouse epididymis. *Biol Reprod* 2013; **89**:1–10.
61. Alvau A, Battistone MA, Gervasi MG, Navarrete FA, Xu X, Sánchez-Cárdenas C, De la Vega-Beltran JL, Da Ros VG, Greer PA, Darszon A, Krapf D, Salicioni AM et al. The tyrosine kinase FER is responsible for the capacitation-associated increase in tyrosine phosphorylation in murine sperm. *Development* 2016; **143**:2325–2333.
62. Battistone MA, Alvau A, Salicioni AM, Visconti PE, Da Ros VG, Cuasnicú PS. Evidence for the involvement of proline-rich tyrosine kinase 2 in tyrosine phosphorylation downstream of protein kinase A activation during human sperm capacitation. *Mol Hum Reprod* 2014; **20**:1054–1066.
63. Visconti PE, Johnson LR, Oyaski M, Fornés M, Moss SB, Gerton GL, Kopf GS. Regulation, localization, and anchoring of protein kinase a subunits during mouse sperm capacitation. *Dev Biol* 1997; **192**:351–363.
64. Zippin JH, Chen Y, Nahirney P, Kamenetsky M, Wuttke MS, Fischman DA, Levin LR, Buck J. Compartmentalization of bicarbonate-sensitive adenylyl cyclase in distinct signaling microdomains. *FASEB J* 2003; **17**:82–84.
65. Baxendale RW, Fraser LR. Mammalian sperm phosphodiesterases and their involvement in receptor-mediated cell signaling important for capacitation. *Mol Reprod Dev* 2005; **71**:495–508.
66. Valsecchi F, Konrad C, D'Aurelio M, Ramos-Espiritu LS, Stepanova A, Burstein SR, Galkin A, Magranè J, Starkov A, Buck J, Levin LR, Manfredi G. Distinct intracellular sAC-cAMP domains regulate ER Ca^{2+} signaling and OXPHOS function. *J Cell Sci* 2017; **130**:3713–3727.
67. Wertheimer E, Krapf D, de la Vega-Beltran JL, Sánchez-Cárdenas C, Navarrete F, Haddad D, Escoffier J, Salicioni AM, Levin LR, Buck J, Mager J, Darszon A et al. Compartmentalization of distinct cAMP signaling pathways in mammalian sperm. *J Biol Chem* 2013; **288**:35307–35320.